XII International Conference on Textile Composites and Inflatable Structures
STRUCTURAL MEMBRANES 2025
R. Wüchner, A. K. Goldbach, R. Rossi and C. Lázaro (Eds)

PARAMETRIC STUDY OF THE MECHNICAL BEHAVIOUR OF MEMBRANE TENSEGRITY STRUCTURES

L. FERRAGU*, J. REBECK* AND R. OVAL*

* Laboratoire Navier
Ecole Nationale des Ponts et Chaussées (ENPC)
6 avenue Blaise Pascal, Cité Descartes, 77455 Champs-sur-Marne, Marne-la-Vallée Cedex2, France
e-mail: julien.rebeck@eleves.enpc.fr, web page: https://ecoledesponts.fr/

Key words: Inflatable structure, Synclastic surface, Gaussian curvature

Summary. Membrane tensegrity structures combine Kenneth Snelson's principles of tensegrity with the potential to create spatial enclosures through continuous envelopes. Current knowledge does not yet support architectural applications of such systems. This article aims to propose a new constructive approach, model their behavior, and identify key parameters of these structures. The focus shifts from traditional form-finding to a form-fitting logic.

1 INTRODUCTION

Tensegrity is a fascinating structural system that has captivated architects and engineers for over 70 years. Yet, it has struggled to find its place in architecture. Membrane tensegrity could be a solution to the architectural problem by combining structure and envelope. Its aesthetic results directly from the expression of forces and materials, much like Félix Candela's shells or Frei Otto's nets. Since the MOOM Pavilion (2011) by the Kojima lab [1], research on this topic has intensified to bring these structures to an architectural scale. The understanding of membrane tensegrity remains rudimentary. The link between the resulting form and the design process has not been questioned. In this article, we attempt to take a step sideways from the current state of the art to propose a new design typology and describe its behavior [3].

2 STATE OF THE ART AND LIMITATIONS

2.1 Membrane tensegrity construction through the deformation of monoclastic surfaces

The current construction method goes from the deformation of a flat plane to a resulting geometry [2]. The struts are placed in a flat membrane, and then the supports are constrained (fig.1a). The membrane has to deform to find a new equilibrium (fig.1b) [3].

The problem is that this process cannot lead to a structure stiff enough for an architectural application. Two approaches are possible. On the one hand, Lycra is used to allow for large displacements and reach a double-curvature surface. The problem is the resulting flexibility of the structure (fig.1a). On the other hand, stiffer material such as PTFE or PVC are used but cannot reach a doube-curvature surface from a single flat element. The resulting structure follows a monoclastic surface [4], less stable under asymetrical load [5].

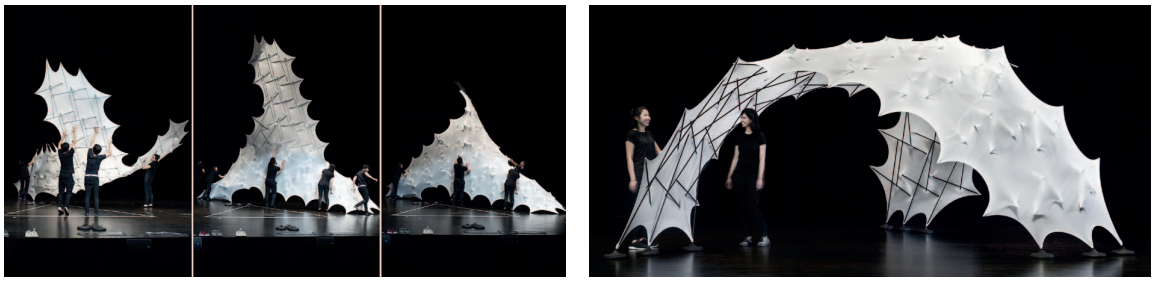

(a) Construction process (b) Resulting structure

Figure 1: Images of the Knit tensegrity shell[3]

We name the different elements that make this structural system shown in fig. 2:

1. membrane tensegrity: a system in equilibrium, given some boundary conditions, with a continuous membrane and a discontinuous set of struts;
2. strut: a straight element in compression put into the membrane;
3. module: two crossed and disjoined struts;
4. opening aperture: space between modules;
5. engagement length: extension length of a module strut in the surface of the next module.

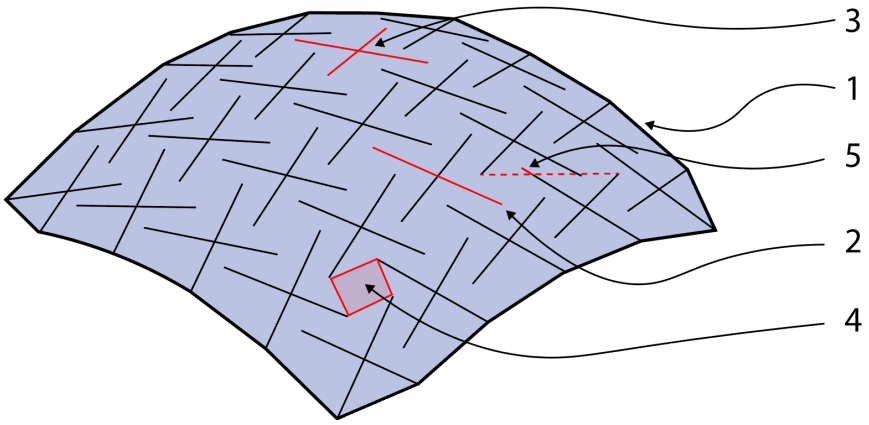

Figure 2: Definition of the different elements in a membrane tensegrity structure

2.2 Analogy with inflatable structures and interest in synclastic target surface

During a previous Master's thesis[6], it has been demonstrated that *form-fitting* of synclastic surfaces increase structural stiffness. This idea was first described by René Motro[7]. Tensegrity can be seen as a discrete inflatable structure. This analogy is still true for membrane tensegrity. As demonstrated in fig. 3, applying a prestress in the struts results in a normal force in the membrane. This is visible in the physical model because these areas are tensioned, even without struts inside.

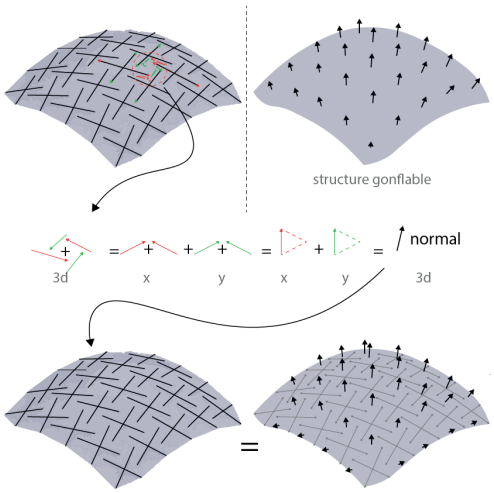

(a) Nodal normal force

(b) Tensioned area in the physical model

Figure 3: Prestressed struts and resulting force, normal to the surface[6]

An inflatable surface, with a convex boundary, is a constant-mean curvature surface, and more particularly, a synclastic surface. For this article, we therefore focus on the value of selecting a synclastic target surface associated with a stiff membrane. We will explore the numerical modeling of this system, then investigate the parameters governing the structural behavior, before discussing the possibility of scaling this type of structure.

3 NUMERICAL MODEL

3.1 Isogeometrical analysis method

For the structural modeling, we used the Isogeometric Analysis (IGA) method. This method employs splines and NURBS within the finite element method. By working with a continuous geometry, we thus circumvent the issues associated with surface meshing[8]. For the form-finding step, we define the initial surface, which we will approximate, along with the position of the struts and the support conditions, which are pinned. The numerical parameters are the prestress in the membrane, the distributed load on the surface, and the description of the struts (materials and cross-sections).

The analysis of the results focuses on the following aspects:

- **Deflection:** We measure the deflection as the distance between the highest point of the strut in the target surface and its position after form-finding.
- **Forces in the struts:** The struts are pin-ended and subjected solely to axial forces. By neglecting geometric imperfections, we discard moment components and the associated buckling phenomena and eccentricities. We evaluate the forces in the struts from their longitudinal strain ϵ using:

$$F = \sigma S = ES\epsilon \tag{1}$$

with $\sigma = E\epsilon$ the axial stress, E the Young modulus and $\epsilon = \frac{L_1 - L_0}{L_0}$ the strain between the initial length L_0 and the final length L_1.

3.2 Validation of the numerical model against a physical model

To validate our numerical model, we compare it to a small-scale physical model. The model is 1.35m long and 0.5m wide. The boundary curves are circular arcs, with radii of 0.2 m and 0.4 m, respectively. Nine modules are arranged along the length and five across the width. The self-weight is estimated at 3 N/m^2. As the prestress is applied by manually inserting and extending the struts within the fabric, its value is estimated at 0.3 kN/m, as follows. To construct the model, we extended as much as possible the strut, without breaking the eyelet. The announced resistance of this eyelet was 3kg out of plane. As we put almost 10 elements along 1m, we estimated the prestress as the sum of the force applied at each eyelet.

With these estimated parameters, the numerical model produces a satisfactory result, with an average deviation of $14mm$ and a $6mm$ difference in deflection (fig. 4).

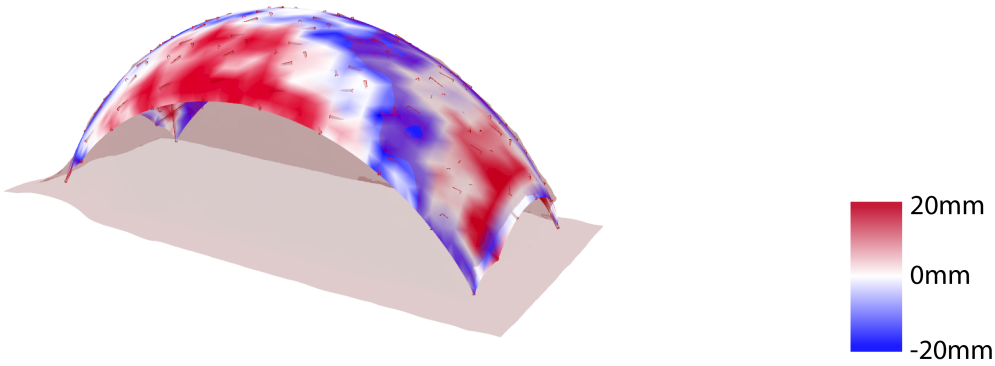

Figure 4: Deviation between the numerical model and the scanned physical model, signed relative to the local normal direction

3.3 Model limitation

The parameters used for the model are the membrane prestress, the application of a distributed load corresponding to the self-weight, and the geometrical and physical description of the struts. The resulting outputs are the final equilibrium state, the deviations, and the strains of the struts. However, the model is just at the form-finding step. So it does not take into account the fabric properties, the welding between to fabric pieces and the concentrated stress at the join between struts and fabric. The estimation of the struts and membrane prestress are also difficult.

4 PARAMETRIC STUDY

For the study of the key parameters of this type of structure, the problem is approached following a design methodology, starting from the most global aspects down to the detailed ones. We therefore address the choice of the target surface based on its curvature, then the tessellation of this

surface, before addressing the consequences between membrane prestress and struts strains. Some parameters are excluded. Geometrical variations are limited to synclastic surfaces. The tessellation patterns remain rudimentary, as the objective is not to address complex topological issues. The stiffness of the membrane is not addressed due to our inability to run a non-linear analysis.

4.1 Gaussian curvature of target surface

In section 2.2, the interest of synclastic surface to create a normal force to the surface has been demonstrated. This section studies the link between stiffness and curvature for a simple synclastic surface. The initial surface is a sphere section, covering a 1m $\times$ 0.5m surface. The hypothesis on the number of modules, loading, and prestress are the same as in section 3.2. We note $\lambda = 1000 f/L$, a ratio between deviation and span, S the covered surface and K the Gaussian curvature (constant on the undeformed sphere).

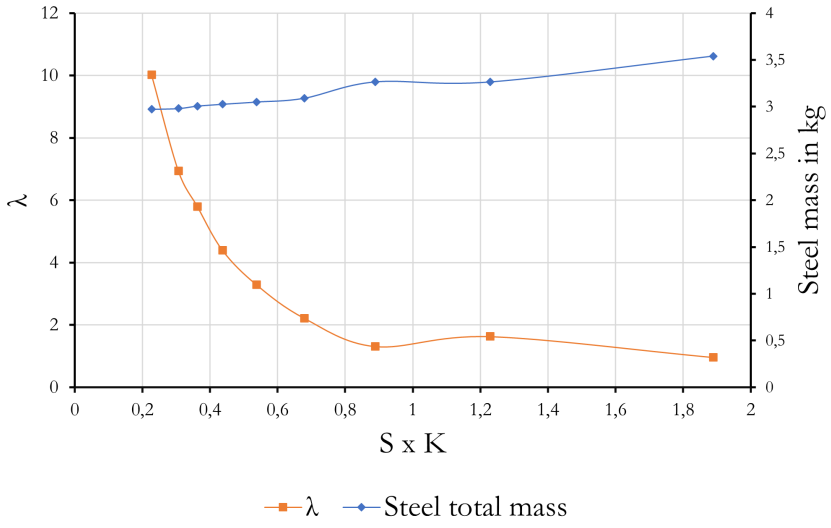

Figure 5: Relation between Gaussian curvature, λ, and steel quantity

Fig. 5 suggests increasing the curvature of the target surface, at least to a certain level, to increase stiffness. The greater the Gaussian curvature, the higher the normal force in the fabric due to prestress. The greater this force, the greater the stiffness of the structure. Nevertheless, it is observed that beyond a ratio of $S \times K = 1$, the reduction in deviation is less significant (-8% when varying from 1 to 1.8) while the quantity of steel continues to increase (+21%). Taking into account the increase in self-weight, an optimum appears to be located around this ratio. Around 1.22, a rebound effect is observed with a loss of stiffness and a quantity of steel that does not increase. For the moment, we cannot explain the reason for this phenomenon. Our hypothesis is that keeping the same engagement length and opening aperture while modifying the curvature leads to an incoherence for surfaces with high curvature.

4.2 Tessellation

4.2.1 Tessellation process

Three different processes were investigated. The first one is a tiling on the xy plane, projected in the z axis on the surface. This process creates a distorted tessellation, the angles are quite deformed. So this method does not give a uniform tessellation to generate a constant prestress. The second one is by using remapping method, with improved results. This method however does not allow the tessellation to be adapted to curvature variations of the surface, creating a large disparity in strut lengths. Finally, the selected method operates directly on the surface. Based on a uniform quad mesh on the surface, the struts are generated given a rotation angle around the face normal (fig 6).

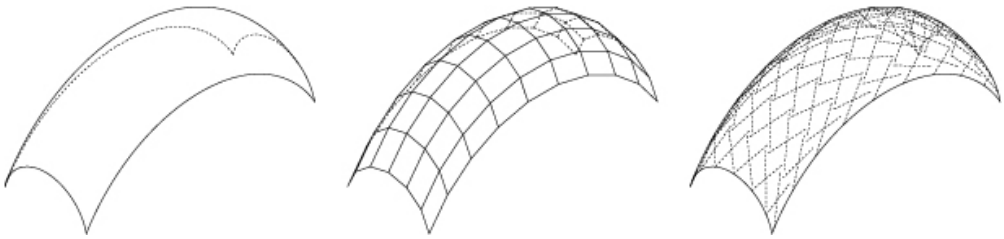

Figure 6: Selected tessellation process: target surface, quad mesh, module in each quad

4.2.2 Tessellation density

After defining a robust tessellation method, the mesh density relative to the overall surface is addressed. We study a sphere section with a radius R = 0.6 m, covering an area of 1 m $\times$ 0.5 m. The opening aperture is fixed at 3 cm. The structure is loaded under its self-weight of 3 N/m^2, and the membrane has an isotropic pretension of P_1=P_2=0.3kN/m. The number of modules is varied uniformly in both directions to preserve, as much as possible, the orientation of the struts. We study a constant ratio between the number of modules in the longitudinal direction n and in the transverse direction m so that $n/m = 2,5$ (see fig. 7). We study the dimensionless factor λ as a function of the ratio between the mean area of one module and the total area, named tessellation density.

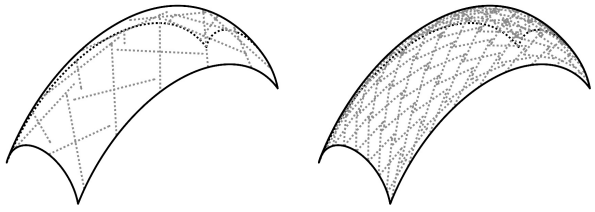

Figure 7: Variation on tessellation density with an homothetic ratio

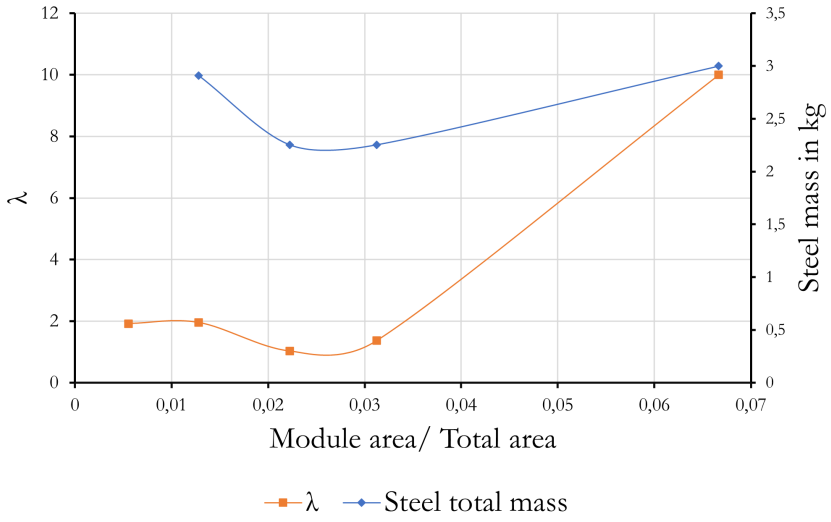

Figure 8: Relation between tessellation density, λ, and steel quantity

Three trends can be observed in figure 8. First, when the modules are very large relatively to the covered surface, the structure exhibits a lower stiffness. This flexibility is explained by the low discretization of the surface, which prevents a homogeneous global behavior. Next, the behavior is optimal, around A_{module}/A_{tot} = 0.025. With further discretization of the surface, the stiffness decreases. Indeed, we can also describe membrane tensegrity structures as reciprocal structures with flexible connections. The relative flexibilities between modules accumulate and end up having a detrimental effect.

4.3 Prestress and stress path

The final parameter studied is the effect of prestress on the distribution of internal forces. All other parameters being equal, we compare two structures (fig 9). For the first one, the prestress in each direction is set to $P_1 = P_2 = P_{min} = 0.3kN/m$, which is the minimum value required to ensure structural stability. For the second one, we set $P_1 = P_2 = 10P_{min} = 3kN/m$.

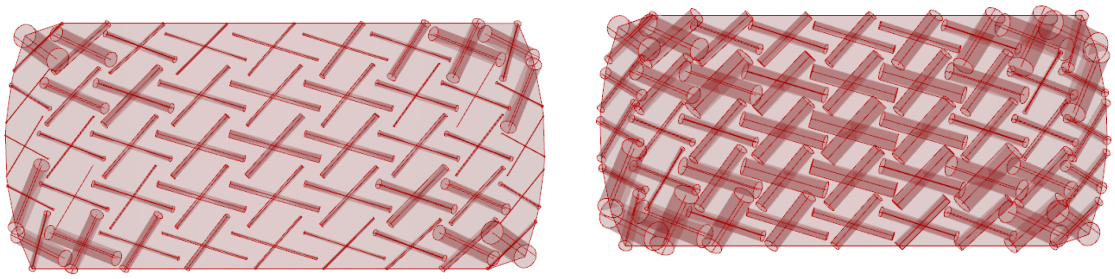

(a) Forces in the strut with $P_{min} = 0.3kN/m$ (b) Forces in the strut with $P = 3kN/m$

Figure 9: Link between axial force and prestress. The higher the axial force, the larger the bar, with a range of axial forces between $F_{min} = 0kN$ and $F_{max} = 0.47kN$

A uniformization of the forces in the struts is observed under an increase of membrane prestress. There is a ratio of 75 between the minimum and maximum axial forces when P_{min} is applied, whereas this ratio is only of 6 with $P = 10P_{min}$. As a consequence of multiplying the prestress by 10, the maximum axial force in the struts increases by 25%. The deflection, meanwhile, decreases by 37% from 1.52 mm to 0.96 mm. This result fosters maximizing the prestress to minimize deformation and uniformize the force flow. For a given strut diameter, it is beneficial to increase the prestress to the maximum that a strut can withstand, while respecting the tensile strength of the membrane. As advised in the French regulations, the prestress should not exceed 6% of the tensile strength so that it can support external loads[9].

5 UP-SCALING THE PROBLEM

5.1 Up-scaling and limitation

The issues raised by increasing the span of the structure are numerous. The first relates to the force in the struts. By applying a scaling factor of 10, the buckling length L_f of the struts increases by the same factor. The critical buckling load for a strut, according to Euler's formula, is divided by 100 in the equation:

$$F_{Euler} = \frac{\pi^2 EI}{L_f^2} \tag{2}$$

Considering that prestress and area are proportionally linked, the forces related to prestress are multiplied by 100. So to avoid buckling, the inertia should be multiplied by 10,000. And we know that the inertia is linked to the radius R of a tube with a thickness e by:

$$I \approx \pi R^3 e \tag{3}$$

So the radius will be also multiplied by $10000^{1/3} = 21$, the area of the section, which is proportional to the perimeter, by 21 and the self-weight also by 21. With a more significant self-weight, the analysis would need to be performed again to verify that the structure finds an equilibrium position and that the tensile strength is not reached in the membrane. However, it is known that to

compensate for a greater self-weight, larger forces must be applied in the membrane. This would bring us back to the previous point (fig 10). Beyond a certain size, we are therefore certainly in the presence of a negative feedback loop that may or may not converge to a valid design (fig. 10). Another issue is the implementation of high prestress. The higher it is, the more complex the construction tools required and the more difficult the construction process becomes for the insertion of the struts.

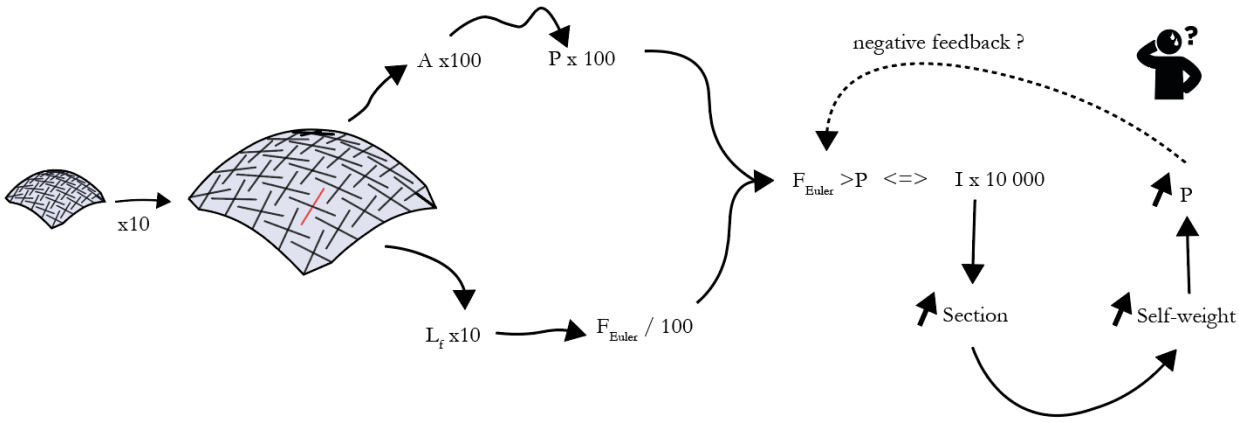

Figure 10: Up-scaling and negative feedback loop

5.2 Structural adaptations to the architectural scale

When studying the behavior of our structure, a more flexible zone appears at the edge. It is not restrained, and the reciprocity of the modules to ensure tension is absent. We therefore wish to strengthen it. One option is the installation of a continuous boundary cable that would run along the entire perimeter of the structure. It would increase the stiffness of the edge of the structure, improve its performance, notably by facilitating the flow of forces at the edge towards the supports. The stiffness of the structure would also increase. The idea emerged from the initial numerical models. We were unable to obtain convergence, and this cable improved the structural behavior, facilitating the convergence of the model. Subsequently, the models were improved and the convergence was reached without these cables. Eventually, the cables were removed to match the behavior of the small-scale physical model. Another option for structural adaptation is a fixed connection of the struts at the center of each module (fig 11). The fixed connection would transform the modules composed of two disjointed struts into a four-branched assembly. It would reduce the buckling length of each strut and thus increase the load-bearing capacity without having to modify the cross-section. Each branch, with a length of L/2 relative to a full strut, would be partially clamped on one end and pinned on the other. However, this connection is difficult to build as the two struts are not in the same plane.

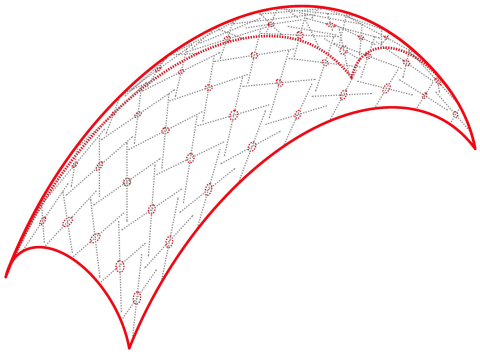

Figure 11: Up-scaling the structure and structural adaptations : strut connection, edge cable

6 CONCLUSION AND PERSPECTIVES

This article proposed and demonstrated the value of a new design approach for membrane tensegrity structures. This approach is based on the use of synclastic surfaces, the use of a stiff membrane, and the generation of the tessellation directly on the target surface. It has enabled the development of a numerical model that captures the behavior of the small-scale physical model. The performance regarding durability and deformation is better compared to membrane tensegrity systems with flexible fabric and single curvature. The different parameters for characterizing the mechanical behavior of the structure were studied to understand its structural behavior. Finally, investigation on scaling up the model was carried out. This step raised several issues, such as self-weight-prestress interactions, and highlighted the need for structural adaptations if the covered surface area is to be increased. On the other hand, the stiffness of the membrane were not accounted for in the models, and the stresses within it are not precisely known. From the geometrical point of view, the surface to target is still an open question. Regarding the discrete inflatable structure analogy, the CMC geometry seems to be an interesting study axis [10]. Besides, the relation between the tessellation and the principal stress curves should be discussed in order to improve the load path. Three points for future research are identified to improve the model. The first is the integration of membrane stresses in the non-linear large displacement analysis, the second is the construction of a larger-scale physical model for further validation of the model, and the third is the consideration of external loads in addition to self-weight, notably asymmetric loads.

REFERENCES

[1] Kojima, Kazujiro. *MOOM*. Tokyo, Japan: Kazujiro Kojima, 2011. Published in *ARQ (Santiago)*, no. 87, August 2014, pp. 40–43. doi: 10.4067/S0717-69962014000200006.

[2] Gupta, S. S., et al. "Exploring Spatial Membrane Tensegrity Shell Structures." *Proceedings of the IASS Annual Symposium*, 2019. https://www.researchgate.net/publication/341204085_Tensile_Configurations_Exploring_Spatial_Membrane_Tensegrity_Shell_Structures

[3] Gupta, S. S., Tracy, K. J., et al. "Prototyping Knit Tensegrity Shells: A Design-to-Fabrication Workflow." *SN Applied Sciences*, vol. 2, 2020, article 1442. doi: 10.1007/s42452-020-2693-4.

[4] Tan, Ying Yi, Tracy, Kenneth J., and Yogiaman, Christine. "Towards Upscaling Membrane Tensegrity Shells: A Design-to-Fabrication Workflow." *Proceedings of the IASS 2023 Symposium*, Melbourne, Australia, 2023. International Association for Shell and Spatial Structures (IASS), 2023. https://www.ingentaconnect.com/contentone/iass/piass/2023/00002023/00000018/art00003;jsessionid=ueku185mm1ps.x-ic-live-03

[5] Nagano, Yohei, and Nagai, Takuo. "Form-Finding and Structural Modeling of Membrane-Tensegrity Composite Structures with Proposal for Highly Feasible Model." In: *Proceedings of the IASS 2024 Symposium: Redefining the Art of Structural Design*, Zurich, Switzerland, August 26–30, 2024. Eds. Philippe Block, Giulia Boller, Catherine DeWolf, Jacqueline Pauli, Walter Kaufmann. International Association for Shell and Spatial Structures (IASS), 2024. https://app.iass2024.org/files/IASS_2024_Paper_289.pdf

[6] Rebeck, J., et al. *Master's Thesis*. École d'architecture de la ville et des territoires Paris-Est, 2022.

[7] Motro, René. *Tensegrity: Structural Systems for the Future*. Hermes Science Publishing, 2003, pp. 36–41. ISBN: 978-1903398076.

[8] Bauer, Anna Maria. "CAD-Integrated Isogeometric Analysis and Design of Lightweight Structures." Doctoral dissertation, Technische Universität München, 2020. ISBN: 978-3-943683-54-7. URL: http://mediatum.ub.tum.de/?id=1540855.

[9] Stranghöner, N., Uhlemann, J., Bilginoglu, F., Bletzinger, K.-U., Bögner-Baltz, H., Corne, E., Gibson, N., Gosling, P., Houtman, R., Llorens, J., Malinowsky, M., Marion, J.-M., Mollaert, M., Nieger, M., Novati, G., Sahnoune, F., Siemens, P., Stimpfle, B., Tanev, V., and Thomas, J.-C. *Prospect for European Guidance for the Structural Design of Tensile Membrane Structures*. Edited by M. Mollaert, S. Dimova, and A. Pinto. Luxembourg: Publications Office of the European Union, 2023. doi: 10.2760/24763. JRC 132615.

[10] Tellier, Xavier, Hauswirth, Laurent, Douthe, Cyril, and Baverel, Olivier. "Discrete CMC Surfaces for Doubly-Curved Building Envelopes." In: *Advances in Architectural Geometry (AAG 2018)*, 2018. https://hal.science/hal-01984201/file/Tellier%20et%20al%202018_Discrete%20CMC%20surfaces%20for%20douby-curved%20building%20envelopes.pdf